Supporting Information

Dynamics of a Supramolecular Capsule Assembly with Pyrene

Hao Tang[1], Carla Santos de Oliveira[1], Gage Sonntag[1], Corinne L.D. Gibb[2], Bruce C. Gibb*[2], Cornelia Bohne*[1]

[1]Department of Chemistry, University of Victoria, PO Box 3065, Victoria, BC V8W 3V6, Canada. [2]Department of Chemistry, Tulane University, New Orleans, LA 70118, USA

Index

Experimental details. *Materials:* OA samples ($C_{96}O_{32}H_{64}{\cdot}4H_2O$) were synthesized as previously described.[1] Py (Aldrich, 99%) was recrystallized at least twice from ethanol:water 9:1 and its purity was checked by single photon counting. A mono-exponential decay indicated that the sample was pure. Sodium tetraborate ($Na_2B_4O_7{\bullet}10H_2O$, BDH, ≥ 98%), sodium iodide (NaI, Aldrich, 99.999%) and methanol (Caledon Laboratories, spectra grade, > 99.8%) were used without further purification. Deionized water (≥ 17.8 MΩ cm^{-1}) from a Barnstead NANOpure system was used for all aqueous solutions.

Solution preparation: Aqueous solutions were prepared as 10 mM borate buffer solutions (pH 8.9). The OA stock solution (555 μM) was prepared by dissolving OA in the buffer solution, while the Py stock solution (1 mM) was prepared in methanol. Solutions at lower OA and Py concentrations were prepared by injecting the appropriate amount of the stock solutions in the buffer solutions. All experiments were performed with aerated solutions, since use of deaerated samples for stopped-flow experiments was not possible. Samples for steady-state and time-resolved fluorescence studies were placed in 10 mm × 10 mm quartz cells and were thermostatized to 20.0 ± 0.1 °C for at least 15 min before experiments were conducted.

Equipment and methods: A Cary 1 or Cary 100 was used to measure UV-Vis absorption spectra. A PTI QM-2 fluorimeter was used to measure steady-state fluorescence spectra. The bandwidths for the excitation and emission monochromators were set to 2 nm. Emission spectra were collected between 350 nm and 500 nm for excitation wavelengths of 335 nm or 340 nm. Excitation spectra were collected between 280 nm and 360 nm for an emission wavelength of 390 nm. The peaks for Py in the excitation spectra are sharp and the precision for the wavelength position on the fluorimeter can vary slightly between days. For this reason, the wavelength position in the excitation spectra was corrected to the peak wavelength in the absorption spectra by applying a wavelength offset. Fluorescence spectra were corrected by subtracting a baseline spectrum collected for solutions that contained all chemicals with the exception of Py. This correction is required to eliminate the solvent Raman emission and any low intensity impurity emission from the sample. The corrected spectra were integrated between 350 nm and 500 nm.

Time-resolved fluorescence experiments were performed with an OB920 single-photon counter from Edinburgh Instruments. The samples were excited either with a flash lamp (331 nm, 16 nm bandwidth) or with a light emitting diode (335 nm, EPLED330). The emission was collected either at 385 nm or 391 nm with a bandwidth for the emission monochromator of 16 nm. The number of counts in the channel of maximum intensity was 2,000. A tail fit was employed since the Py excited state lifetime is much longer than the instrument response function. The decays were fit to a mono-exponential function, where k_{obs} is the decay rate constant for the singlet excited state of pyrene, which corresponds to the inverse of the Py excited state lifetime. The quality of the fits was judged from the χ^2 value, which should be between 0.9 and 1.2, and from the randomness of the residuals between the calculated and experimental values.[2] A short-lived emission defined by 1 or 2 channels in the decay was sometimes observed and is likely due to a low intensity emission from OA, since such decay was not observed in the absence of OA. The presence of this short decay did not change the Py lifetime measured.

$$I(t) = I_0 \, e^{-k_{obs} t} \qquad \text{(S1)}$$

Stopped-flow experiments were performed with a SX20 system from Applied Photophysics. The excitation source was a Hg-Xe lamp (L2382-Hamamatsu Photonics) and the slit bandwidth for the excitation monochromator was 0.19 nm for both excitation wavelengths (335 nm and 340 nm). The position of the excitation monochromator was determined by measuring the dependence of the background intensity for a cell containing water with the wavelengths reading on the monochromator and comparing the intensity maxima with the principle emission maxima of the specifications for the Hg-Xe lamp provided by the manufacturer. Any offset was used to position the monochromator at 335 nm or 340 nm. The emission from the sample was collected using an interference filter with maximum transmission at 405 nm (FWHM of 38 nm, Melles Griot, lot 13637, ANDV7248). The excitation and emission optics are in an orthogonal arrangement. The samples were thermostated at 20.0 ± 0.1 °C for 15 min and were then mixed in a 1:1 ratio. The concentrations stated for the stopped-flow experiments are final concentrations and correspond to half of the concentrations of chemicals in each syringe. The same photomultiplier voltage, leading to an output voltage lower than 6 V, was employed throughout one experiment to ensure that fluorescence intensities could be compared. At least 20 individual kinetic traces were averaged. The control experiments performed were: Mixing of buffer with buffer or OA solution with buffer, both of which yielded the same intensity value. This value is the baseline value for the experiment. The mixing of Py with buffer was used to

determine the intensity for Py in the absence of OA. A straight line was observed for this experiment as expected since the dilution of Py is fast and occurs within 1 ms.

The kinetic data were either analyzed as single kinetics by fitting the data to an exponential decay (eq. S2) or growth (eq. S3) or by using a global analysis method where all kinetic traces were fit simultaneously to a kinetic model using the non-linear least-squared regression method in Pro-Kineticist 2 from Applied Photophysics.

$$I_t = (I_0 - I_\infty)\, e^{-k_{obs}\, t} + I_\infty \qquad (S2)$$

$$I_t = (I_\infty - I_0)\left(1 - e^{-k_{obs}\, t}\right) + I_0 \qquad (S3)$$

I_o and I_∞ are respectively the intensities at time zero and when the kinetic trace has leveled off and k_{obs} is the first-order observed rate constant. For the purpose of comparing different kinetic traces and determining K_{11}, the intensities were corrected by subtracting the baseline intensities. In addition, these corrected intensities were normalized by dividing by the corrected intensity of Py in water.

Absorption and fluorescence properties of Py complexed to OA.

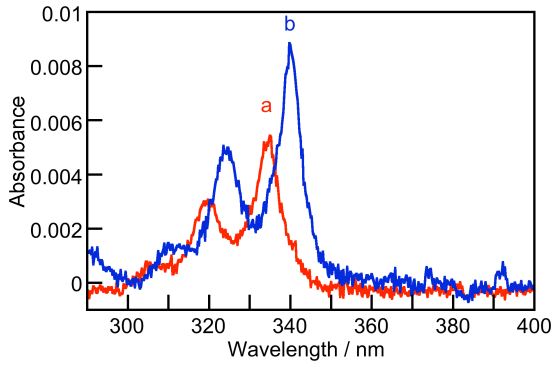

Figure S1. Absorption spectra for the borate buffer solutions of 0.2 μM Py in the absence (a, red) and presence of 4 μM OA (b, blue) The spectra were corrected by subtracting a baseline which corresponds to the absorbance for a mixture containing all chemicals with the exception of Py.

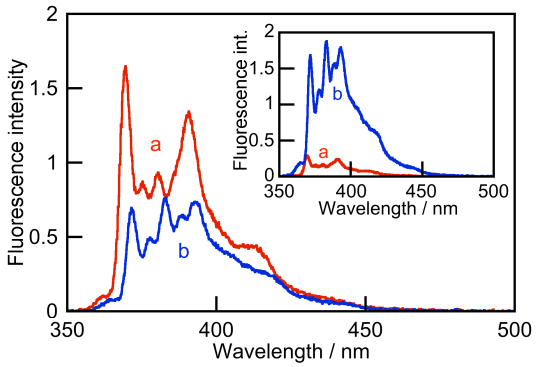

Figure S2. Fluorescence emission spectra for the buffer solutions of 0.2 μM Py in the absence (red) and presence of 4 μM OA (blue). The excitation wavelengths were respectively set at 335 nm and 340 nm for the spectra shown in the main figure and for the spectra in the inset.

Quenching of excited Py by iodide anions.

The singlet excited state of Py is quenched efficiently by iodide anions.[3] Quenching leads to an increase in the observed decay rate constant for the excited state and the quenching rate constants were obtained from equation S4:

$$k_{obs} = k_o + k_q\,[\text{iodide}] \qquad (S4)$$

The quenching plots in the absence and presence of excess OA were linear and the recovered quenching rate constants were $(1.1 \pm 0.2) \times 10^9$ M^{-1} s^{-1} for Py in buffer and $(5.9 \pm 0.7) \times 10^5$ M^{-1} s^{-1} for Py in the OA capsule. Since the reaction in homogeneous solution is close to a diffusion-controlled process, the rate constant in the presence of OA is related to the access of iodide anions to Py within the capsule.

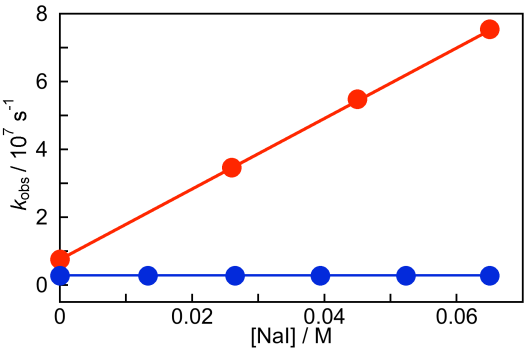

Figure S3: Stern Volmer plots for the quenching of the singlet excited state of Py (λ_{ex} = 331 nm, λ_{em} = 385 nm) in buffer (red, [Py] = 0.5 μM) and in the presence of OA (blue, [Py] = 0.5 μM, [OA] = 20 μM). The lines represent the fit of the experimental data to equation S4.

Binding isotherm for the formation of the 2:1 OA-Py complex. The dependence of I_{flu} on the OA concentration was fit numerically using Scientist 3 from Micromath. An equation is defined for I_{flu} as a function of emission efficiencies and the concentrations of Py in the aqueous phase ([G]) or bound to OA as OA-Py 2:1 complex ([H_2G]). The relationship between the concentrations of various Py and OA species is defined by the overall equilibrium binding constant for the OA-Py 2:1 complex (β_{21}, Scheme S1) and the mass balance equations (eqs. S7 and S8).

$$\mathrm{Py} + 2\mathrm{OA} \overset{\beta_{21}}{\rightleftharpoons} \mathrm{OA \cdot Py \cdot OA} \qquad \text{(S5)}$$

Scheme S1. Overall equilibrium for the formation of the OA•Py•OA complex.

The model employed in Scientist 3 is as follows: The total concentration of OA ($[H]_T$) is defined as the independent variable. The equilibrium concentrations of free host ([H]), free guest ([G]), 2:1 complex ([H_2G]) and the fluorescence emission intensity (I_{Flu}) are defined as dependent variables. The relative emission efficiency for the 2:1 complex (C_{21}), which corresponds to the ratio of the emission efficiency for Py in the OA•Py•OA complex and in water, and the overall equilibrium binding constant for the 2:1 complex (β_{21}) are defined as parameters. *R*, the ratio of the fluorescence emission intensity of Py in the absence of OA ($I_{flu,0}$) to the total concentration of Py ($[G]_T$), is a constant for each independent experiment.

The equations for this model are listed as follows:

$$[H_2G] = \beta_{21} \times [G] \times [H]^2 \qquad \text{(S6)}$$

$$[H] = [H]_T - 2 \times [H_2G] \qquad \text{(S7)}$$

$$[G] = [G]_T - [H_2G] \qquad \text{(S8)}$$

$$I_{flu} = R \times ([G] + C_{21} \times [H_2G]) \qquad \text{(S9)}$$

$$R = \frac{I_{flu,0}}{[G]_T} \qquad \text{(S10)}$$

Ranges for the dependent variables are listed as follows:

$$0 < [H] < [H]_T \qquad \text{(S11)}$$

$$0 < [G] < [G]_T \qquad \text{(S12)}$$

$$0 < [H_2G] < [G]_T \qquad \text{(S13)}$$

The fluorescence spectra at various OA concentrations are shown in figure S4. The β_{21} value determined by fitting the binding isotherm (Fig. 2 in the paper) from the average of two independent experiments is (3.19 ± 0.06) × 10^{12} M^{-2}. The errors for the β_{21} values recovered from each experiment are smaller than the average deviation for the average from two independent experiments. The error stated is the average deviation.

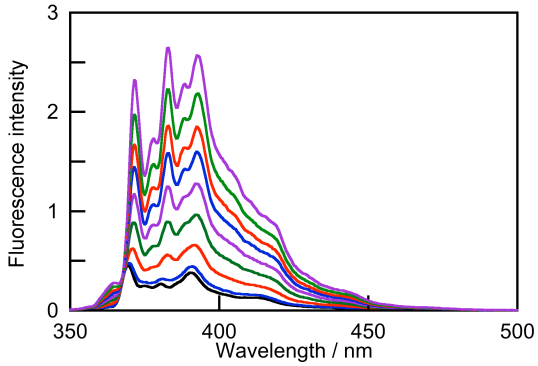

Figure S4. Dependence of the fluorescence emission spectra of Py (λ_{ex} = 340 nm) on the concentration of OA. [Py] = 0.2 μM; [OA] from bottom to top are: 0 μM, 0.09 μM, 0.28 μM, 0.46 μM, 0.65 μM, 0.83 μM, 1.02 μM, 1.48 μM and 5.13 μM. The intensity increases with the increase in the OA concentration.

Binding isotherm for the formation of the 1:1 OA-Py complex. The dependence of the fluorescence intensities (I_{11}) from stopped-flow or steady-state fluorescence experiments on the OA concentration was fit numerically using Scientist 3 from Micromath. The measured variable is defined as a function of the concentrations of Py species and the emission efficiencies for these species. The relationship between the concentrations of Py and OA is defined by the equilibrium binding constant for the 1:1 complex (K_{11}) and the mass balance equations (eqs. S15 and S16).

The model employed in Scientist 3 is as follows: The total concentration of OA ($[H]_T$) is defined as the independent variable. The equilibrium concentration of free host ([H]), free guest ([G]), 1:1 complex ([HG]) and I_{11} are defined as the dependent variables. The relative emission efficiency for the 1:1 complex (C_{11}) compared to the efficiency for free Py, and the overall equilibrium binding constant for the 1:1 complex (K_{11}) are defined as parameters in the model. *R*, the ratio of the fluorescence intensity of Py in the absence of OA ($I_{11,0}$) to the total concentration of Py ($[G]_T$), is a constant for

each independent experiment. The value of R is dependent on the settings on the fluorimeter and varies between experiments, while C_{11} is constant between experiments.

The equations for this model are listed as follows:

$$[HG] = K_{11} \times [G] \times [H] \quad \text{(S14)}$$

$$[H] = [H]_T - [HG] \quad \text{(S15)}$$

$$[G] = [G]_T - [HG] \quad \text{(S16)}$$

$$I_{11} = R \times ([G] + C_{11} \times [HG]) \quad \text{(S17)}$$

$$R = \frac{I_{11,0}}{[G]_T} \quad \text{(S18)}$$

Ranges for the dependent variables are listed as follows:

$$0 < [H] < [H]_T \quad \text{(S19)}$$

$$0 < [G] < [G]_T \quad \text{(S20)}$$

$$0 < [HG] < [G]_T \quad \text{(S21)}$$

The binding isotherm for the changes in the steady-state fluorescence intensity (Fig. S4) with the concentration of OA did not fit to a model where only a 1:1 OA:Py complex is formed at equilibrium (Fig. S5). This result is expected because of the formation of the 2:1 OA:Py complex.

The transient formation of the 1:1 complex was observed in the stopped-flow experiments and the fit of the intensity for the fast process, i.e. step function in the kinetic trace, was fit with the model for a 1:1 complex (Fig. S6). The K_{11} value determined was $(4.5 \pm 0.6) \times 10^5$ M^{-1} by fitting combined data from two independent experiments. The error stated was recovered from the fitting routine.

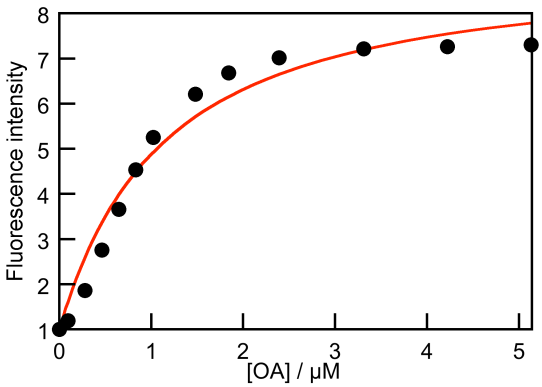

Figure S5. Binding isotherm for the complexation of Py (0.2 μM, λ_{ex} = 340 nm) with OA in borate buffer determined from the changes in the steady-state fluorescence intensity fit to a 1:1 Py-OA complexation model.

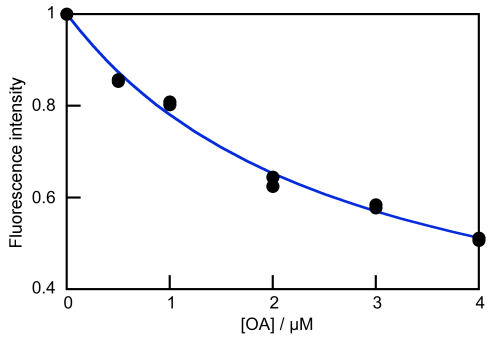

Figure S6. Dependence of the offset intensity change measured by stopped-flow with the concentration of OA ([Py] = 0.2 μM, λ_{ex} = 335 nm).

Stopped-flow kinetics and relationship of its amplitude to the intensity changes in the steady-state fluorescence measurements.

The kinetics for the formation of the OA•Py•OA complex were followed as a change in the fluorescence intensity when the solution was excited at 335 nm. This excitation wavelength led to a decrease in the Py emission intensity because the molar absorptivity for OA•Py•OA at 335 nm is smaller than the molar absorptivity for free Py (Fig. S1). Excitation at 335 nm was chosen over excitation at 340 nm because of the higher intensity of the Hg-Xe lamp at 335 nm. The same observed rate constants were obtained for samples excited at 335 nm or 340 nm showing that the kinetics were not dependent on the excitation wavelengths. The decays leveled off within 10 s (Fig. S7) and the normalized amplitude for the intensity change in the stopped-flow experiment is the same as the normalized intensity change in the steady-state fluorescence study (Fig. S8). This latter result indicates

that the kinetics for capsule formation is finished within 10 s.

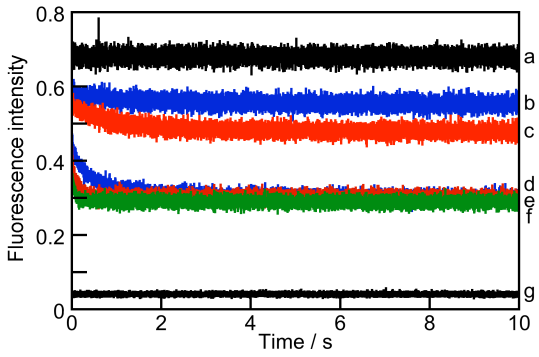

Figure S7. Stopped-flow kinetics for the change in the Py emission (λ_{ex} = 335 nm) when Py was mixed with OA ([Py] = 0.2 μM. [OA] = 0 μM (a, black), 0.5 μM (*b*, blue), 1 μM (*c*, red), 2 μM (*d*, blue), 3 μM (*e*, red) and 4 μM (*f*, green). The control experiment of buffer mixing with buffer is shown in trace g.

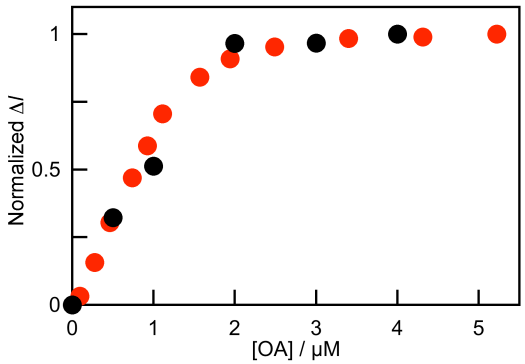

Figure S8. Dependence for the changes in the emission intensity (ΔI) measured by steady-state fluorescence (●, red) or stopped flow (●, black) with the addition of OA to 0.2 μM Py in buffer. The intensity changes at the highest OA concentrations were normalized to 1.

Analysis of the stopped-flow kinetics. The analysis presented is for the data set shown in figure 3 in the paper and figure S7 above. The decays fit to a mono-exponential function (Fig S9 and S10).

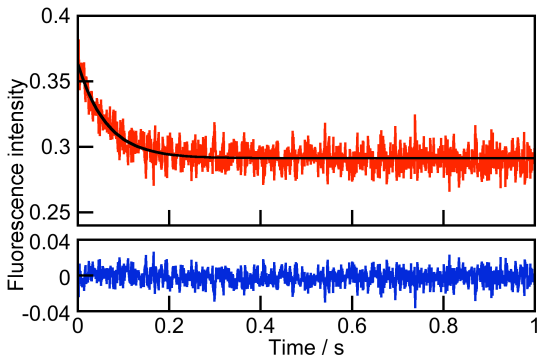

Figure S9. Stopped flow trace *f* (Fig. S7) fit with a mono-exponential function (black, top panel) for 0.2 μM Py mixing with 4 μM OA (red). Bottom panel: Residuals between the calculated and the experimental data (blue). Only the first 1 s of the trace *f* is shown since the intensity leveled off in this time window.

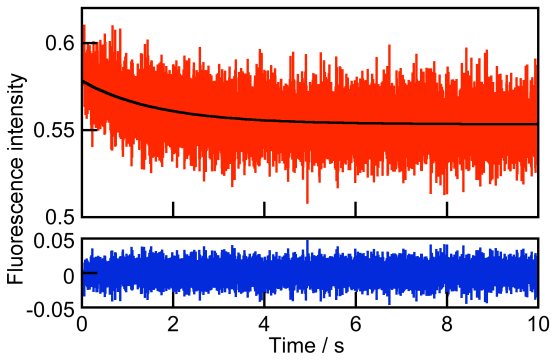

Figure S10. Stopped flow trace *b* (Fig. S7) fit with a mono-exponential function (black, top panel) for 0.2 μM Py mixing with 0.5 μM OA (red). Bottom panel: Residuals between the calculated and the experimental data (blue).

Global analysis was employed to fit the kinetic traces obtained at variable OA concentrations to a model where the Py•OA complex is formed in pre-equilibrium and the formation kinetics of the OA•Py•OA complex is observed as a relaxation process (Scheme 1 in the paper). The residuals for this fit were random. Similar k_{21}^{+} values, (2.59 ± 0.09) × 10^6 $M^{-1}s^{-1}$ and (2.39 ± 0.09) × 10^6 $M^{-1}s^{-1}$, were recovered from two independent experiments, while the k_{21}^{-} values were not reproducible and had large errors, suggesting that the value for k_{21}^{-} and/or the amplitude for the dissociation process are too low for an accurate determination of this rate constant. Therefore the kinetics were fit by assuming that the formation of the 2:1 complex is irreversible (Scheme S2). The residuals for this fit were also random (Fig. S11). The k_{21}^{+} values recovered, (2.58 ± 0.07) × 10^6 $M^{-1}s^{-1}$ and (2.63 ± 0.02) ×

10^6 $M^{-1}s^{-1}$, were the same as when including k_{21}^- in the model. If the removal of k_{21}^- was not warranted then non-random residuals for the model without k_{21}^- and different k_{21}^+ values for the two fitting models would have been obtained. The fit to the mechanism in Scheme S2 was repeated by varying the K_{11} values from 3.9×10^5 M^{-1} to 5.1×10^5 M^{-1} (Table S1), which correspond to the upper and lower limits considering the error for the K_{11} value. The average for k_{21}^+ from two independent experiments was $(2.6 \pm 0.2) \times 10^6$ M^{-1} s^{-1}. The error stated for the averaged k_{21}^+ value corresponds to an error propagation from individual values, since these errors were equal or larger than the average deviation.

$$OA + Py \underset{}{\overset{K_{11}}{\rightleftharpoons}} OA{\bullet}Py \qquad (S22)$$

$$OA + OA{\bullet}Py \xrightarrow{k_{21}^+} OA{\bullet}Py{\bullet}OA \qquad (S23)$$

Scheme S2. Reactions for the binding of Py with OA in the presence of buffer.

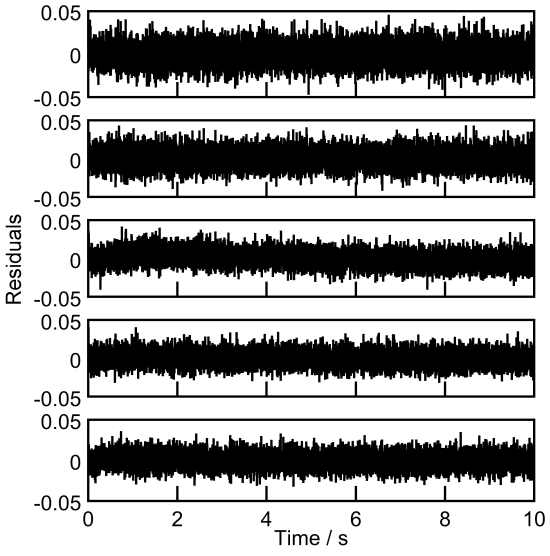

Figure S11. Residuals between the experimental data (Fig. S7) and the calculated best-fit values according to the model shown in Scheme S2. [Py] = 0.2 μM; [OA] from top to bottom are: 0.5 μM, 1 μM, 2 μM, 3 μM and 4 μM.

Table S1. Association rate constant values for the formation of OA•Py•OA complex (k_{21}^+) recovered from the global fitting for various fixed K_{11} values.

K_{11} / 10^5 M^{-1}	k_{21}^+ / 10^6 M^{-1} s^{-1}	
	trial I	trial II
3.9	2.79 ± 0.07	2.84 ± 0.03
4.5	2.58 ± 0.07	2.63 ± 0.02
5.1	2.44 ± 0.06	2.47 ± 0.02

[a]The errors were recovered for the globally fits of the kinetic traces using the model shown in Scheme S2.

References.

(1) Gibb, C. L. D.; Gibb, B. C. *J. Am. Chem. Soc.* **2004**, *126*, 11408.

(2) Bohne, C.; Redmond, R. W.; Scaiano, J. C. In *Photochemistry in Organized and Constrained Media*; Ramamurthy, V., Ed.; VCH Publishers: New York, **1991**, 79.

(3) Chen, M.; Grätzel, M.; Thomas, J. K. *J. Am. Chem. Soc.* **1975**, *97*, 2052.